Title page

C-type natriuretic peptide improves maternally aged oocytes quality by inhibiting excessive PINK1/Parkin-mediated mitophagy

Running title: CNP improves oocytes quality

Hui Zhang[1, 2a], Chan Li[1, 2a], Qingyang Liu[1, 2], Jingmei Li[1, 2], Hao Wu[1, 2], Rui Xu[1, 2], Yidan Sun[1, 2], Ming Cheng[1, 2], Xiaoe Zhao[1, 2], Menghao Pan[1, 2], Qiang Wei[1, 2b], Baohua Ma[1, 2b]

1 College of Veterinary Medicine, Northwest A&F University, Yangling, Shaanxi, People's Republic of China,

2 Key Laboratory of Animal Biotechnology, Ministry of Agriculture, Yangling, Shaanxi, People's Republic of China

[a] These authors contributed equally.

[b] Corresponding author: Baohua Ma and Qiang Wei

Address: College of Veterinary Medicine, Northwest A&F University, Yangling, Shaanxi, People's Republic of China; Key Laboratory of Animal Biotechnology, Ministry of Agriculture, Yangling, Shaanxi, People's Republic of China. 712100

Email: mabh@nwsuaf.edu.cn (Baohua Ma); weiq@nwsuaf.edu.cn (Qiang Wei).

Abstract

The overall oocyte quality declines with ageing, and this effect is strongly associated with a higher reactive oxygen species (ROS) level and the resultant oxidative damage. C-type natriuretic peptide (CNP) is a well-characterized physiological meiotic inhibitor that has been successfully used to improve immature oocyte quality during in vitro maturation (IVM). However, the underlying roles of CNP in maternally aged oocytes have not been reported. Here, we found that the age-related reduction in the serum CNP concentration was highly correlated with decreased oocyte quality. Treatment with exogenous CNP promoted follicle growth and ovulation in aged mice and enhanced meiotic competency and fertilization ability. Interestingly, the cytoplasmic maturation of aged oocytes was thoroughly improved by CNP treatment, as assessed by spindle/chromosome morphology and redistribution of organelles (mitochondria, the endoplasmic reticulum [ER], cortical granules [CGs], and the Golgi apparatus). CNP treatment also ameliorated DNA damage and apoptosis caused by ROS accumulation in aged oocytes. Importantly, oocyte RNA-seq revealed that the beneficial effect of CNP on aged oocytes was mediated by restoration of mitochondrial oxidative phosphorylation, eliminating excessive mitophagy. CNP reversed the defective phenotypes in aged oocytes by alleviating oxidative damage and suppressing excessive PINK1/Parkin-mediated mitophagy. Mechanistically, CNP functioned as a cAMP/PKA pathway modulator to decrease PINK1 stability and inhibit Parkin recruitment. In summary, our results demonstrated that CNP supplementation constitutes an alternative therapeutic approach for advanced maternal

age-related oocyte deterioration and may improve the overall success rates of clinically assisted reproduction in older women.

Keywords: C-type natriuretic peptide; oocyte meiosis; embryo; antioxidant; mitophagy

INTRODUCTION

During growth, oocytes gradually acquire the capacity to resume meiosis, complete maturation, undergo successful fertilization and achieve subsequent embryo developmental competence (Gandolfi & Gandolfi, 2001). However, ovarian involution precedes that of any other organ in female mammals, and in humans, the oocyte fertilization rate decreases rapidly after 35 years of age. Indeed, infertility associated with a decline in oocyte quality with increasing maternal age is a significant challenge.

Recently, with the development of cultural and social trends, many women have delayed childbearing, and ovarian senescence has become a public health problem (Bartimaeus, Obi, Igwe, & Nwachuku, 2020; Broekmans, Soules, & Fauser, 2009). Ovarian ageing is accompanied by abnormalities in organelle distribution, morphology and functions, leading to inadequate oocyte growth, maturation, fertilization and subsequent embryo development (Reader, Stanton, & Juengel, 2017). Consequently, assisted reproductive technologies such as in vitro maturation (IVM) and in vitro fertilization (IVF) have become promising options for infertility treatment (Chang, Song, Lee, Lee, & Yoon, 2014). However, further studies are needed to improve the subsequent developmental competence of maternally aged oocytes.

Oocyte maturation has two steps: nuclear maturation, which mainly involves germinal vesicle breakdown (GVBD) and chromosomal segregation, and cytoplasmic maturation, which involves redistribution of organelles (mitochondria, cortical granules [CGs], and the endoplasmic reticulum [ER]), changes in the intracellular ATP and antioxidant contents, and the accumulation of fertilization-related transcripts and proteins (McClatchie et al., 2017; Watson, 2007). The quality and developmental potential of aged oocytes are lower than those of oocytes derived from young females, primarily because aged oocytes exhibit negative consequences of cytoplasmic maturation, such as abnormal mitochondria and an aberrant CG distribution (Miao, Cui, Gao, Rui, & Xiong, 2020), deteriorated organelle and antioxidant system function and increased reactive oxygen species (ROS) levels (T. Zhang et al., 2019). Excessive ROS generation leads to destructive effects on cellular components (Zarkovic, 2020). Notably, recent studies have indicated that increased oxidative damage is closely correlated with the occurrence of mitochondrial damage and mitophagy (Jiang et al., 2021), which is accompanied by blockade of oocyte meiosis (Jin et al., 2022; Q. Shen, Liu, Li, & Zhang, 2021).

The endogenous C-type natriuretic peptide (CNP) produced by follicular mural granulosa cells as a ligand of natriuretic peptide receptor 2 (NPR2), which is expressed primarily in cumulus cells, plays a crucial role in maintaining meiotic arrest (Meijia Zhang, Su, Sugiura, Xia, & Eppig, 2010). Recent studies have suggested that CNP, an inhibitor of oocyte maturation, provides adequate time for cytoplasmic maturation, offering a new strategy to optimize the synchronization of nuclear and

cytoplasmic maturation and improve the quality of immature oocytes in vitro (Wei et al., 2017). Moreover, CNP has been reported to enhance the antioxidant defence ability and developmental competence of oocytes in vitro (Zhenwei & Xianhua, 2019). Therefore, CNP may constitute a new alternative means to enhance antioxidant system function and protect against oxidative damage by eliminating excess ROS in aged oocytes. Although CNP has been suggested to contribute to improving the maturation and subsequent development of immature mouse oocytes in vitro, the effect of CNP on maternally aged oocytes remains to be determined.

In this study, we investigated the redistribution and function of organelles (mitochondria, CGs, and the ER), the ATP content and the intracellular GSH level in CNP-treated maternally aged oocytes. The results showed that CNP improves the cytoplasmic maturation and developmental competence of maternally aged oocytes by optimizing organelle distribution and function and inhibiting PINK1/Parkin-mediated mitophagy. The findings of this study will contribute to understanding the mechanism of CNP in increasing the fertilization capacity and developmental ability of aged oocytes.

RESULTS

CNP supplementation improves the quality of aged oocytes

To explore the effect of CNP on oocyte quality in aged mice, we first investigated whether intraperitoneal injection of CNP can affect oocyte quality. Young and aged mice were hormonally superovulated after 14 days of consecutive PBS or

CNP daily injection (Figure 1A, B). As shown in Fig. 1 C-E, body weights were higher but ovary weight and the ratios of ovary to body weight were lower in the aged mice as compared with their young counterparts. However, ovary weight and the ratios of ovary to body weight of the CNP-treated mice were significantly recovered (Fig. 1 D and E). Serum CNP concentrations were measured in young, aged, and aged + CNP injected mice. The endogenous CNP content in serum from aged mice was markedly lower than that in serum from young mice (Figure 1 F). In contrast, administration of CNP to aged mice significantly elevated the CNP content in serum (Figure 1 F). To further determine whether the elevated CNP content in serum can improve oocyte quality, we evaluated the number, first polar body (PB1) extrusion rate and fragmentation rate. As the mice aged, the number of ovulations and the PB1 extrusion rate decreased significantly, but the incidence of fragmented oocytes increased dramatically (Figure 1 G-J). Conversely, CNP supplementation apparently ameliorated the ageing-induced defects in the number and morphology of the ovulated oocytes (Figure 1 G-J). In addition, assessment of follicle development in the ovary sections by HE staining showed severe deterioration of follicles at different developmental stages in aged mice; however, CNP supplementation significantly increased the number of secondary follicles and antral follicles (Figure 1 K and L). Young, untreated aged and CNP-treated aged mice were naturally mated with 12-week-old male mice, and consistent with the increased number of ovulated oocytes with a normal morphology, the litter size of aged mice was also increased by CNP administration (Figure 1M).

To investigate the effects of CNP on in vitro maturation (IVM) of aged mouse cumulus-oocyte complexes (COCs), we first examined the PB1 extrusion rate of COCs pretreated with 10 nM CNP to maintain meiotic arrest for 24 h (pre-IVM) and then matured in vitro for 16 h (a two-step culture system; Figure S1 A). In the control (conventional in vitro maturation) group, only 35.36 ± 2.74% of the oocytes exhibited PB1 extrusion. After temporary meiotic arrest induced by treatment with 10 nM CNP, the maturation rate increased to 71.12 ± 3.02% (n=104), significantly higher than that in the control group ($P<0.01$) (Figure S1 B and C). The spindle morphology and chromosome alignment in in vitro-matured oocytes were also evaluated. The percentage of oocytes with abnormal spindle-chromosome complexes was significantly decreased in the group with 10 nM CNP-induced temporary meiotic arrest (Figure S1 D and E). Collectively, these results indicate that CNP administration increased the serum CNP content, restored the number and morphology of aged oocytes and improved the fertility of aged female mice.

CNP supplementation restores cytoplasmic maturation events in maternally aged mouse oocytes

Pregnancy failure and foetal miscarriage increase with maternal age and, importantly, are associated with oocyte aneuploidy and spindle/chromosomal abnormalities (Ma et al., 2020). Therefore, we determined the rate of spindle/chromosomal abnormalities in oocytes of young, untreated aged and CNP-treated aged mice by immunofluorescence staining and found that CNP treatment greatly improved the spindle/chromosomal abnormalities in aged mice (Figure 2 A, B).

To determine whether, in addition to affecting spindles/chromosomes, CNP supplementation affects other organelles during the maturation of aged oocytes, we examined the distribution of the Golgi apparatus, endoplasmic reticulum (ER) and cortical granules (CGs) in oocytes from young, untreated aged and CNP-treated aged mice. The Golgi-Tracker results showed that in aged mouse oocytes, the Golgi apparatus was distributed in agglutinated and clustered patterns, and CNP supplementation significantly reduced the rate of abnormal Golgi distribution (Figure 2 C, D, Figure S2A, B). Since the ER plays an essential role in Ca^{2+} signal-mediated oocyte fertilization and subsequent embryonic development (Miyazaki & Ito, 2006), we then examined the distribution pattern of the ER in oocytes. As shown in Figure 2 E, the ER was accumulated at the chromosome periphery and was evenly distributed in the cytoplasm; however, the ER abnormally agglomerated in the cytoplasm and the chromosome periphery in a disorganized pattern in aged oocytes (Figure 2 E, Figure S3A). Statistical analysis showed that the rate of abnormal ER distribution was significantly decreased in CNP-supplemented oocytes (Figure 2 F, Figure S3B). The distribution of CGs is one of the most important indicators of oocyte cytoplasmic maturation and is related to the blockade of polyspermy following fertilization. We assessed whether CNP supplementation affects the distribution dynamics of CGs in aged oocytes. Lens culinaris agglutinin (LCA)-FITC staining showed that in young oocytes, CGs were distributed evenly in the oocyte subcortical region, leaving a CG-free domain (CGFD) near chromosomes (Figure 2 G). However, maternally aged oocytes showed an abnormal CG distribution, including increased migration of CGs

176 towards the oocyte chromosomes or oocyte subcortical region, without leaving a
177 CGFD (Figure 2 G, H; Figure S4 A). Consistent with this finding, statistical analysis
178 of the fluorescence intensity of CG signals in aged oocytes showed a significant
179 reduction compared with that in young oocytes, and CNP supplementation improved
180 the mis-localization and decrease in the number of oocyte CGs (Figure 2 H, I, Figure
181 S4 B, C). Taken together, these data imply that CNP is a potent agent for improving
182 cytoplasmic maturation events in maternally aged mouse oocytes.

183 **CNP supplementation restores mitochondrial distribution and function in aged**
184 **oocytes**

185 To verify the effect of CNP supplementation on the mitochondrial distribution
186 pattern and function in aged oocytes, we performed MitoTracker staining. In young
187 oocytes, mitochondria exhibited a homogeneous distribution in the cytoplasm and
188 accumulated at the periphery of chromosomes (Figure 2 J). However, in aged oocytes,
189 most mitochondria were aggregated in the cytoplasm and partially or completely
190 failed to accumulate around chromosomes (Figure 2 J, Figure S5A). Statistically,
191 more than 40% of mitochondria in aged oocytes exhibited a mislocalized distribution
192 pattern, and CNP supplementation significantly reduced the abnormal distribution rate
193 (Figure 2 K, Figure S5B). We then analysed mitochondrial function by measuring the
194 ATP content in oocytes from young, untreated aged, and CNP-treated aged mice. The
195 ATP content in oocytes from aged mice was considerably lower than that in oocytes
196 from young mice but was restored following CNP supplementation (Figure 2 L,
197 Figure S5C). We also tested the mitochondrial membrane potential, which has been

shown to be the driving force of mitochondrial ATP synthesis, by staining with the potentiometric dye JC-1 (Figure 2 M, Figure S5D). The mitochondrial membrane potential was lower in oocytes from aged mice than in oocytes from young mice but was restored in oocytes from CNP-supplemented aged mice (Figure 2 M, N, and Figure S5 D, E). Overall, these observations suggest that CNP supplementation improved ageing-induced mitochondrial dysfunction in oocytes.

CNP supplementation eliminates excessive ROS and attenuates DNA damage and apoptosis in aged oocytes

We proposed that mitochondrial dysfunction induces ROS imbalance and oxidative stress in aged oocytes. To test this hypothesis, we carried out dichlorofluorescein (DCFH) staining to measure ROS levels in each group of oocytes (Figure 3 A). Quantitative analysis of the fluorescence intensity showed that ROS signals were markedly enhanced in aged oocytes compared with young oocytes (Figure 3 B). Conversely, CNP supplementation effectively reduced the ROS accumulation observed in aged oocytes (Figure 3 A, B, Figure S6A, S6B). In addition to being caused by ROS accumulation, age-associated oxidative stress damage can be caused by reduced antioxidant defence system function. We therefore investigated whether CNP contributes to improving the antioxidant defence ability in aged oocytes. Quantification of the nicotinamide adenine dinucleotide phosphate (NADPH) levels and the ratio of reduced to oxidized glutathione (GSH/GSSG ratio) in oocytes showed that NADPH levels and the GSH/GSSG ratio were decreased in oocytes from aged mice compared with those from young mice and that CNP treatment significantly

increased NADPH levels and the GSH/GSSG ratio in oocytes from aged animals (Figure 3 C, D). Because a high level of ROS not only results in the accumulation of DNA damage but also causes oocyte apoptosis (Miao et al., 2020), we next evaluated DNA damage and apoptosis in oocytes by γ-H2A.X and Annexin-V staining, respectively. As expected, higher signals indicating DNA damage and apoptosis were observed in aged oocytes than in young oocytes, and these increases were alleviated by supplementation with CNP (Figure 3 E-H). Taken together, these observations suggested that the rates of DNA damage and apoptosis are higher in aged oocytes, possibly because of maternal ageing-induced excessive accumulation of ROS. Notably, our results demonstrated that CNP supplementation exerts antioxidant activity, which is an effective strategy to ameliorate maternal ageing-induced DNA damage and apoptosis in oocytes.

CNP supplementation improves the fertilization ability and early embryo development of aged oocytes

Considering that oocyte fertilization and subsequent embryo developmental competence are profoundly affected by mitochondrial function, we then tested whether the oocyte fertilization capacity and normal development to the blastocyst stage are enhanced by CNP. The in vitro fertilization (IVF) results showed that aged oocytes had dramatically lower fertilization rates than young oocytes and that CNP supplementation effectively increased the fertilization rate of aged oocytes (Figure 4 A, B). We further examined the subsequent developmental ability of the fertilized oocytes. As expected, CNP supplementation effectively increased the blastocyst

formation rate of aged oocytes both in vivo (Figure 4 A and 4 C–F) and in vitro (Figure S7). These results demonstrate that CNP increases the fertilization capacity and promotes subsequent embryonic development of oocytes from aged mice.

Identification of target effectors of CNP in aged oocytes by single-cell transcriptome analysis

To verify the cellular and molecular mechanisms of CNP supplementation in improving oocyte quality in aged mice, we performed single-cell transcriptome analysis of GV oocytes derived from young, untreated aged and CNP-treated aged mice to identify potential target effectors. The relative expression of several randomly selected genes from each group was verified using quantitative real-time PCR (Figure S8A, B). As shown in the heatmap and volcano plot, the transcriptome profile of aged oocytes was significantly different from that of young oocytes, with 77 differentially expressed genes (DEGs) downregulated and 440 DEGs upregulated in aged oocytes identified through DEGseq2 analysis (Figure 5 A-C). Furthermore, CNP supplementation resulted in downregulation of 584 genes and upregulation of 527 genes compared with aged oocytes. In particular, Kyoto Encyclopedia of Genes and Genomes (KEGG) enrichment analysis showed that genes enriched in the ubiquitin-mediated proteolysis and mitophagy pathways were abnormally highly expressed in aged oocytes compared with young oocytes but that these expression levels were restored to the baseline levels in CNP-supplemented aged oocytes (Figure 5 D, E). In addition, oxidative phosphorylation and peroxisome proliferator-activated receptor (PPAR) signalling pathways were ranked at the top of the enrichment list in CNP-

supplemented aged oocytes compared to untreated aged oocytes, consistent with our abovementioned observations that CNP supplementation improved mitochondrial function in aged oocytes. Many of the enriched KEGG enrichment pathways are highly related to mitophagy and mitochondrial function, which suggests that mitophagy should be strongly considered as a CNP effector in aged oocytes.

CNP supplementation attenuates oxidative damage by inhibiting mitophagy in aged oocytes

To verify the effect of CNP supplementation on mitophagy in aged oocytes, we first analysed mitochondrial structure in the oocytes of young, untreated aged and CNP-treated aged mice by transmission electron microscopy (Figure 6 A). Quantitatively, mitochondrial damage, as evidenced by membrane rupture and a lack of electron density was significantly increased in aged oocytes but was ameliorated in CNP-supplemented aged oocytes (Figure 6 B). Because oxidative stress has been implicated in triggering mitochondrial oxidative injury and mitophagy (Adhikari, Lee, Yuen, & Carroll, 2022; M. Shen et al., 2016), we next determined whether supplementation with CNP can eliminate excessive mitochondrial ROS (mtROS). As expected, supplementation with CNP substantially reduced the mtROS signals, as shown by MitoSOX staining and fluorescence intensity measurements (Figure 6 C, D). We then evaluated degradation of the autophagy biomarker p62, the accumulation of LC3-II, the conversion of LC3-I to LC3-II, and the expression patterns of the mitophagy-related proteins PINK1 and Parkin (Figure 6 E). Western blot analysis revealed that aged oocytes exhibited significant p62 degradation, LC3-II

accumulation and marked increases in PINK1 and Parkin expression levels, whereas CNP supplementation abrogated these effects (Figure 6 E-I). Collectively, the above data indicate the inhibitory effect of CNP on oocyte mitophagy through the PINK1-parkin signalling pathway.

CNP downregulates Parkin recruitment and mitophagy via the cAMP/PKA pathway

How PINK1- and Parkin-mediated mitophagy is regulated by CNP in aged oocytes, however, requires further elucidation. The cAMP/PKA signalling pathway, which is dependent on the phosphorylation of mitochondrial proteins, has emerged as a direct means to regulate mitophagy and mitochondrial physiology (Amer & Hebert-Chatelain, 2018; Lobo et al., 2020). The concentrations of cAMP in GV oocytes derived from young, untreated aged and CNP-treated aged mice were determined. As shown in Fig. 6 J, the cAMP concentration in aged oocytes was significantly lower than that in young oocytes, but administration of CNP resulted in a substantial increase in intraoocyte cAMP concentrations. This increase in cAMP significantly reduced mitochondrial recruitment of Parkin and mitophagy, which were dependent on PKA activity (Lobo et al., 2020). Next, we applied a PKA inhibitor, H89, to determine whether PKA is directly involved in CNP-mediated oocyte mitophagy. We isolated preantral follicles (80-100 μm diameter) from the ovaries of aged mice and treated them with 100 nM CNP or 100 nM CNP + 10 μM H89 during in vitro culture. Monitoring of follicle growth dynamics showed that treatment with 100 nM CNP significantly increased the follicle diameter (Figure 6 K and L), whereas H89

treatment inhibited the effect of CNP on promoting preantral follicle growth (Figure 6 K and L). Western blot analysis revealed that CNP supplementation significantly decreased PINK1 and Parkin expression levels, but H89 treatment abrogated these expression changes (Figure 6 M-O). The cAMP-PKA pathway plays an important role in inhibiting Parkin recruitment to damaged mitochondria (Akabane et al., 2016). We therefore sought to determine whether PKA inhibition regulates Parkin recruitment. The effects of CNP on mitochondria were examined by double staining for Parkin and translocase of outer mitochondrial membrane 20 (TOMM20). CNP clearly inhibited the mitochondrial localization of Parkin, but inhibition of PKA with H89 resulted in Parkin translocation to mitochondria, as shown by the overlap of the two staining signals (Figure 6 P and Q). Collectively, these data suggested that the suppression of Parkin recruitment through the cAMP-PKA axis is an important mechanism underlying the protective effect of CNP against oxidative injury in maternally aged mouse oocytes.

DISCUSSION

In mammals, the endogenous peptide CNP is expressed by endothelial cells in many tissues and has diverse physiological functions in mediating cardioprotective effects, bone growth, oocyte meiotic progression, and follicle growth and development (Bae et al., 2017; Moyes & Hobbs, 2019; Peake et al., 2014; Sato, Cheng, Kawamura, Takae, & Hsueh, 2012; Xi et al., 2019). Beyond the role of CNP as an oocyte meiotic arrest factor, previous studies by our group and others confirmed that adding CNP to the pre-IVM system significantly improved oocyte maturation and

subsequent embryo developmental potential (Richani & Gilchrist, 2022; Soto-Heras, Paramio, & Thompson, 2019; Wei et al., 2017). The synchronization of nuclear and cytoplasmic maturation is essential for oocyte quality and supporting early embryonic preimplantation development. However, the underlying molecular mechanism and whether CNP has any beneficial effect on the maternal age-induced decline in oocyte quality are incompletely understood. In the present study, we showed that CNP levels declined with age and demonstrated that CNP supplementation increased the number of antral follicles and the ovulation rate and enhanced oocyte quality and fertility. Furthermore, supplementation of CNP in pre-IVM oocyte culture medium reversed the adverse effects of age on immature oocytes, offering a potentially effective approach for assisted reproductive technologies to acquire a greater number of high-quality oocytes and improve the fertility of older women.

Many factors affect the adverse effects on the oocyte maturation process and embryonic development associated with advanced maternal age (Mikwar, MacFarlane, & Marchetti, 2020). Assisted reproductive technologies are an efficient scheme to resolve infertility as maternal fertility declines with ageing. However, the low success rate of IVM oocytes, which is especially pronounced in maternally aged oocytes, limits fertilization outcomes. Our in vivo results showed that CNP supplementation results in multiple improvements, including reductions in oxidative damage, spindle defects, and abnormal organelle distributions and functions, in maternally aged oocytes. Thus, we further investigated the use of CNP in the IVM system, especially in improving the quality of oocytes derived from aged mice. The results indicated that

CNP-induced temporary meiotic arrest improved the maturation and fertilization rate of maternally aged oocytes and increased their subsequent embryo developmental competence. Specifically, our results confirmed an advanced role for CNP in preventing the development of mitochondrial structure abnormalities and the typical dysfunctional processes in aged oocytes. Furthermore, these data showed that CNP apparently improved the antioxidant defence system impairment accompanying oocyte ageing and alleviated oxidative stress. In addition, the findings demonstrated that CNP improved cytoplasmic maturation events by maintaining normal CG, ER and Golgi apparatus distribution and mitochondria function in aged oocytes.

The asynchronous nature of nuclear and cytoplasmic maturation is a major challenge in improving the quality of IVM oocytes (Coticchio et al., 2015). Age-related aberrant chromosome alignment prior to cytoplasmic maturation may result in poor oocyte quality and subsequent reduced reproductive potential (Russ, Haywood, Lane, Schoolcraft, & Katz-Jaffe, 2022). In the present study, after COCs were induced, the temporary meiotic arrest resulting from CNP treatment significantly increased the maturation rate, which may synchronize oocyte nuclear and cytoplasmic maturation. Organelle distribution is a necessary feature of oocyte cytoplasmic maturation and subsequent development. Dramatic ER reorganization (FitzHarris, Marangos, & Carroll, 2007), CG translocation to the cell cortex (Liu, Sims, Calarco, & Talbot, 2003), and the Golgi apparatus distribution and function are commonly regarded as indicators of cytoplasmic maturation (Mao, Lou, Lou, Wang, & Jin, 2014). Similarly, our results demonstrate that CNP supplementation restored cytoplasmic maturation in

maternally aged oocytes by ensuring normal organelle distribution dynamics and organelle function, increasing the fertilization capacity and developmental competence of aged oocytes. It is reasonable to assume that CNP is a potential option to prevent abnormal organelle distribution and functions in oocytes that could be triggered by ubiquitous environmental endocrine disruptors, such as bisphenol A and citrinin (Pan et al., 2021; Sun et al., 2020). Cortical granules (CGs) are oocyte-specific vesicles located under the subcortex. Fusion of CGs with the oocyte plasma membrane is the most important event needed to prevent polyspermy (Miao et al., 2020). The distribution of CGs is usually regarded as one of the most important indicators of oocyte cytoplasmic maturation. The contents of the CGs are normally discharged by exocytosis when the egg is stimulated by the fertilizing spermatozoon; this process is called the cortical reaction, and it prevents polyspermy and protects the embryo from a hostile environment during early development (Schuel, 1978).

One of the major known causes of oocyte oxidative damage and apoptosis arises from excessive ROS accumulation with ageing, especially in IVM oocytes (Combelles, Gupta, & Agarwal, 2009; Soto-Heras & Paramio, 2020). Excessive ROS accumulation occurs as a result of two processes, namely, constant generation in the mitochondria or scavenging by antioxidant defence systems, both of which involve age-related quality decreases in oocytes (Mianqun Zhang, Lu, Chen, Zhang, & Xiong, 2020). Thus, maintaining the balance between the production and scavenging of ROS could help to alleviate age-related oxidative damage and fertility decreases. Some antioxidative factor(s) within oocytes might deteriorate as the potential mother ages,

compromising the ability for ROS scavenging (Schwarzer et al., 2014). GSH serves as one of the antioxidants in oocytes to combat ROS-mediated oxidative stress, which is highly correlated with oocyte developmental competence (Furnus et al., 2008). The present results suggested that CNP-induced temporary meiotic arrest increased the GSH/GSSG ratio, which is involved in the enhancement of oocyte antioxidant defence and may contribute to improving oocyte developmental competence. Consistent with previous studies (Miao et al., 2020), our findings validated that maternal ageing results in excessive accumulation of ROS and DNA damage, which severely impairs follicle development, ovulation, oocyte quality and subsequent embryo developmental potential.

Defects in chromosome separation and decondensation as well as chromosomal misalignment caused by spindle detachment are the major contributing factors responsible for the decline in oocyte quality with ageing (Chiang, Schultz, & Lampson, 2011; Eichenlaub-Ritter, Vogt, Yin, & Gosden, 2004). Oocytes require ATP for spindle formation, chromosome segregation, and polar body extrusion and fertilization processes (Arhin, Lu, Xi, & Jin, 2018; Eichenlaub-Ritter, 2013). Mitochondria are the most abundant organelles in oocytes and play an important role in ATP production via oxidative phosphorylation to phosphorylate adenosine diphosphate (Bentov, Yavorska, Esfandiari, Jurisicova, & Casper, 2011). Thus, mitochondrial function is a key indicator of oocyte quality and successful fertilization in assisted reproductive technologies (ARTs) (Mikwar et al., 2020). Mitochondrial metabolic activity and mitochondrial DNA replication dramatically decrease in

418 oocytes with maternal age, which reduces ATP production; leads to meiotic spindle
419 damage, chromosome misalignment and aneuploidy; and largely impairs oocyte
420 maturation processes (Eichenlaub-Ritter, Wieczorek, Lüke, & Seidel, 2011; May-
421 Panloup et al., 2016). We demonstrated that CNP reverses mitochondrial dysfunction
422 induced by ageing in oocytes by analysing the mitochondrial distribution, ATP content,
423 and mitochondrial membrane potential (ΔΨm).

424 Notably, disruption of the mitochondrial membrane potential is a potent trigger
425 of mitophagy (Matsuda et al., 2010). Our single-cell transcriptome profiling data
426 showed that the expression of genes related to ubiquitin-mediated proteolysis and the
427 mitophagy pathway was considerably upregulated in aged oocytes but restored to
428 normal levels following CNP supplementation. We also observed by TEM that CNP
429 supplementation suppressed the accumulation of autophagic vesicles containing
430 mitochondria. Furthermore, immunoblot analysis revealed degradation of the
431 autophagy biomarker p62 and accumulation of LC3-II in aged oocytes, events that
432 were markedly suppressed in CNP-treated oocytes. In general, excessive activation of
433 mitophagy and mitochondrial damage in aged oocytes may be involved in the
434 deterioration of oocyte quality, while CNP can ameliorate this process.

435 The PINK1/Parkin pathway is one of the most studied ubiquitin-dependent
436 mitophagy processes and is crucial for the equilibrium between mitochondrial
437 biogenesis and mitochondrial removal via selective recognition and elimination of
438 dysfunctional mitochondria (Ateneo, 2019). In healthy mitochondria, the
439 serine/threonine kinase PINK1 is usually expressed at low levels, but it rapidly

accumulates on damaged or aged mitochondria that exhibit loss of membrane potential (Narendra & Youle, 2011). The decrease in the mitochondrial membrane potential abolishes translocation across the outer and inner membranes and confines PINK1 in the mitochondrial matrix, stabilizing it on the mitochondrial outer membrane in a complex with the translocase TOM (De Gaetano et al., 2021). Stabilized PINK1 recruits the cytosolic E3-ubiquitin ligase Parkin from the cytosol to damaged mitochondria, an event followed by mitophagy. The effects of CNP on meiotic arrest depend on the maintenance of cAMP levels in oocytes (Meijia Zhang et al., 2010). Recent findings revealed that cAMP-dependent activation of PKA reduced the PINK1 protein level due to its rapid degradation via the proteasome and severely inhibited Parkin recruitment to depolarized mitochondria (Lobo et al., 2020). Our data confirmed that PINK1 expression was decreased in CNP-treated oocytes, thus leading to a reduction in Parkin recruitment. However, these effects were disrupted by the inhibition of PKA pathway activity, indicating that cAMP indeed mediates the ameliorating effects of CNP on aged oocyte quality. Taken together, these findings indicate that PKA-mediated inhibition of Parkin recruitment may contribute to protecting mitochondria with a low membrane potential from mitophagy in aged oocytes.

Collectively, our studies demonstrated that CNP improves the fertilization and developmental competence of maternally aged mouse oocytes by preventing age-related antioxidant defects and excessive mitophagy. Considering its known contributions as a physiological meiotic inhibitor, CNP provides an alternative to

prevent maternal age-related oocyte quality defects and improve developmental competence. Although ARTs have been widely used to treat infertility, their overall success rates in women of advanced maternal age remain low. Our data may provide a new theoretical basis for the use of CNP in improving subfertility in older women or the application of clinically assisted reproduction. Out of caution, however, randomized controlled clinical trials should be conducted to further study the efficacy of CNP in women who wish to become pregnant.

MATERIALS AND METHODS

Animals and ethics statement

The young (6~8-week-old) and aged (58~60-week-old) C57BL-6J female mice were obtained from the Experimental Animal Center of the Xi'an Jiaotong University and housed in a temperature (20~25℃) and light-controlled environment (12 h light–12 h dark cycle) and provided with food and water ad libitum.

In vivo treatment with CNP

Aged mice (58-week-old) were intraperitoneally injected daily with CNP (120 μg/kg body weight; Cat#B5441, ApexBio) for 14 days. CNP was dissolved in PBS and diluted to appropriate concentration by physiological saline solution before injection. The mice were followed by a single injection of 5 IU pregnant mare serum gonadotropin (PMSG; Ningbo Second Hormone Factory, Ningbo, China) for 46 h to stimulate penultimate follicle maturation before collection of ovaries for histological analyses and weighting. Some mice were further injected with 5 IU human chorionic

483 gonadotropin (hCG; Ningbo Second Hormone Factory, Ningbo, China), and the
484 ovulated oocytes in oviducts were monitored 16 h later to evaluate ovulation
485 efficiency.

486 **Measurement of CNP levels**

487 CNP was measured in plasma by a two-site polyclonal direct ELISA kit
488 (Biomedica Medizinprodukte, Vienna, Austria) according to the manufacturer's
489 instructions. Collect blood samples in standardized serum separator tubes (SST),
490 allow samples to clot for 30 minutes at room temperature and perform serum
491 separation by centrifugation. Assay the acquired serum samples immediately. Read
492 the optical density (OD) of all wells on a plate reader using 450 nm wavelength.
493 Construct a standard curve from the absorbance read-outs of the standards. Obtain
494 sample concentrations from the standard curve.

495 **Histological analysis of ovaries**

496 Ovaries from each group of mice were fixed in 4% paraformaldehyde (pH 7.5)
497 overnight at 4□, dehydrated using graded ethanol, followed by xylenes and embedded
498 in paraffin. Paraffin-embedded ovaries were serial sectioned at a thickness of 5 μm for
499 hematoxylin and eosin (H&E) staining. Ovaries from three mice of each group were
500 used for the analysis.

501 **Collection and culture of cumulus-oocyte complexes (COCs)**

502 Female mice were stimulated by an intraperitoneal injection of 5 IU PMSG, and

mice were sacrificed by cervical dislocation 24 h later. The ovaries were collected, and the well-developed Graafian follicles were punctured with 30-gauge needles to collect COCs. Only COCs with morphological integrity and a distinct germinal vesicle (GV) were cultured in basic culture medium consisted of Minimum Essential Medium (MEM)-α (Life Technologies, New York, USA) supplemented with 3mg/mL bovine serum albumin and 0.23 mM pyruvate at 37°C under an atmosphere of 5% CO_2 in air with maximum humidity.

CNP treatment and in vitro maturation

For in vitro induce temporary meiotic arrest, COCs were cultured in basic culture medium containing 10 nM of CNP. The dose of CNP for meiotic arrest in mouse oocytes in vitro was selected based on the published literatures (Meijia Zhang et al., 2011) and our preliminary reports (Wei et al., 2017). After meiotic arrest culture for 24 h, COCs were transferred to CNP-free IVM medium (containing 10 ng/mL epidermal growth factor (EGF)) to induce maturation. After incubation for 16 h, COCs were denuded of cumulus cells by treatment with 0.03% hyaluronidase to obtain MII oocytes for future experiments.

In vitro fertilization and embryo culture

Caudae epididymides from 12-week-old male C57BL-6J mice were lanced in a dish of in human tubal fluid (HTF) medium to release sperm, followed by being capacitated for 1 h (37°C under an atmosphere of 5% CO_2 in air with maximum humidity). Maturated oocytes were incubated with capacitated sperm at a

concentration of 4×10^5/mL in 100 μL HTF for 6 h at 37°C, 5% CO_2. The presence of two pronuclei was scored as successful fertilization. The embryos were cultured in KSOM under mineral oil at 37 ℃ in 5% CO_2 and saturated humidity.

Preantral follicle isolation and culture

Ovaries were removed after the animals had been killed by cervical dislocation and preantral follicles were mechanically isolated using 26-gauge needles. Then, the preantral follicles (80–100μm diameter) that enclosed by an intact basal membrane were collected, distributed randomly and cultured individually in 96-well tissue culture plates for up to 6 days at 37°C in a humidified atmosphere of 5% CO_2 in air. The basic culture medium consisted of MEM-α supplemented with 1mg/mL BSA, 1% ITS (5μg/ mL insulin, 5μg/mL transferrin, 5ng/mL selenium; Sigma), 100μg/mL sodium pyruvate and 1% penicillin/streptomycin sulfate (Sigma) in the absence (control) or presence of 100nM CNP or 10 μM H89. The dose of CNP was selected based on the published literatures (Xi et al., 2019). Half the medium was replaced with fresh medium and follicles were photographed every other day, and follicle diameter was measured using ImageJ at each time point.

Immunofluorescent Staining

Oocytes were fixed in 4% paraformaldehyde in PBS for 30 min at room temperature, and permeabilized with 0.5% Triton X-100 for 20 min, then blocked with 1% BSA in PBS for 1 h at room temperature. The oocytes were incubated with primary antibodies (Alexa Fluor® 488 Conjugate anti-α-tubulin monoclonal

antibody,1:200, Cell Signaling, Cat#35652; rabbit anti-Tom20 antibody, 1:100, Cell Signaling, Cat#sc-42406; mouse anti-Parkin antibody, 1:100, Santa Cruz, Cat#sc-32282) at 4°C overnight, and then the oocytes were extensively washed with wash buffer (0.1% Tween 20 in PBS), probed with Alexa Fluor 488 goat anti-rabbit IgG (1:200, Thermo Fisher Scientific, A21206) or Alexa Fluor 594 donkey anti-mouse IgG (1:200, Abcam, ab150108) in a dark room for 1 h at room temperature. Then oocytes were counterstained with DAPI (10 μg/mL) at room temperature for 10 min. Finally, samples were mounted on glass slides and observed viewed under the confocal microscope (Nikon A1R-si).

Mito-Tracker, ER-Tracker, and Golgi-Tracker Red Staining

Oocytes were incubated with Mito-tracker Red (1:2000, Beyotime Biotechnology, Shanghai, China), ER-Tracker Red (1:3000, Beyotime Biotechnology), Golgi-Tracker Red (1:50, Beyotime Biotechnology) in M2 medium for 30 min at 37 °C in a 5% CO_2 and saturated humidity. Then, the oocytes were counterstained with DAPI (10 μg/mL) for 5min at 37 °C in a 5% CO_2 and saturated humidity, and finally, the samples were washed 3 times with M2 medium and examined with a confocal laser-scanning microscope (Nikon A1R-si).

Mitochondrial membrane potential (ΔΨm) measurement

Oocyte mitochondrial membrane potential was evaluated using Mito-Probe JC-1 Assay Kit (Beyotime Institute of Biotechnology, Shanghai, China). Briefly, oocytes were incubated with 2 μM JC-1 in M2 medium for 30 min at 37 °C in a 5% CO_2 and

saturated humidity, and finally, the samples were washed 3 times with M2 medium and examined with a confocal laser-scanning microscope (Nikon A1R-si). JC-1 dye exhibits a fluorescence emission of green (529 nm) and red (590 nm). Thus, the red/green fluorescence intensity ratio was measured to indicate mitochondrial depolarization. Oocytes mitochondrial membrane potential ($\Delta\Psi m$) measurements were performed as our previous report (H. Zhang et al., 2020).

Monitoring of ROS levels in oocytes

The amount of ROS in oocytes was processed with 10 μM oxidation sensitive fluorescent probe dichlorofluorescein (DCFH) (Beyotime Institute of Biotechnology, Shanghai, China) for 30 min at 37□ in M2 medium. Then oocytes were washed three times with M2 medium and placed on glass slides for image capture under a confocal microscope (Nikon A1R-si).

Determination of mitochondrial ROS (mitoSOX) generation by MitoSOX staining, GV oocytes were incubated in M2 media containing 5 μM MitoSOX Red (ThermoFisher, M36008, Waltham, USA,) in humidified atmosphere for 10 min at 37°C. After washing three times in M2 media, oocytes were imaged under a confocal microscope (Nikon A1R-si).

Measurement of the GSH/GSSG ratio

The GSH/GSSG ratio was measured with a GSSG/GSH Assay Kit (Beyotime Institute of Biotechnology) according to the manufacturer's instructions. Briefly, oocytes were lysed in 40 μL deproteinized buffer on ice for 10 min. The lysate was

587 centrifuged at 12000×g for 5 min at 4 °C. For GSSG measurement, the samples were
588 incubated with GSH scavenge buffer for 60 min at 25 °C to decompose GSH. Then,
589 the samples were transferred to the 96-well plates and the absorbance was measured
590 with a multimode plate reader (BioTek Epoch) at 412 nm.

591 **Measurement of the oocyte NADPH content**

592 The oocyte NADPH contents were measured using a NADPH assay kit
593 (Beyotime Institute of Biotechnology) according to the manufacturer's instructions.
594 Briefly, 50 ~ 60 oocytes per group were lysed in 100 μL NADPH extraction buffer on
595 ice for 20 min. After the samples were centrifuged at 12000×*g* for 5 min at 4 °C, the
596 supernatants were transferred to the 96-well plates (50μl per well), and the absorbance
597 was measured using a multimode plate reader (BioTek Epoch) at 450 nm. The amount
598 of NADPH was determined using a calibration curve.

599 **Western blot analysis**

600 Approximately 200 oocytes were lysed in RIPA buffer (solarbio, Beijing, China)
601 that supplemented with 1mM protease inhibitors phenylmethylsulfonyl fluoride
602 (PMSF, solarbio, Beijing, China), on ice for 30 min. Samples were boiled at 100 °C in
603 a metal bath for 10 min in protein loading buffer (CoWin Biosciences, Beijing, China)
604 and equal amount proteins were separated by 10% SDS-PAGE gel, and transferred to
605 polyvinylidene fluoride (PVDF) membranes (Millipore, Bedford, USA). After transfer,
606 the membranes were blocked in TBST that contained 3 % BSA for 1 h at room
607 temperature, followed by incubation with primary antibodies at 4 °C overnight (the

608 primary antibodies were rabbit anti-GAPDH antibody, 1:2000, Cell Signaling,
609 Cat#5174; rabbit anti-p62 antibody, 1:1000, Cell Signaling, Cat#23214; rabbit anti-
610 Tom20 antibody, 1:1000, Cell Signaling, Cat#sc-42406; rabbit anti-LC3A/B antibody,
611 1:1000, Abcam, Cat#ab128025; rabbit anti-PINK1 antibody, 1:1000, Cell Signaling,
612 Cat#6946; mouse anti-Parkin antibody, 1:1000, Santa Cruz, Cat#sc-32282). The
613 secondary antibodies were incubated for 1 h at room temperature, and then the
614 membrane signals were visualized by a chemiluminescent HRP substrate reagent
615 (Bio-rad Laboratories, Hercules, CA, USA) and images were captured with
616 Tanon5200 Imaging System (Biotanon, Shanghai, China). The band intensity was
617 assessed with Image J software and normalized to that of GAPDH.

618 **Transmission electron microscope (TEM)**

619 Oocytes were prefixed with 3% glutaraldehyde, refixed with 1% osmium
620 tetroxide, dehydrated in acetone, and embedded in Ep812 (Can EM Ltd.). Semithin
621 sections were stained with toluidine blue for optical positioning, and ultrathin sections
622 were made with a diamond knife and observed by a JEM-1400FLASH transmission
623 electron microscope (JEOL) after staining with uranyl acetate and lead citrate.

624 **Evaluation of total ATP content**

625 The ATP content of oocytes was detected with an ATP Bioluminescence Assay
626 Kit (Beyotime Institute of Biotechnology). The oocytes were lysed with 50 μl of ATP
627 lysis buffer on ice, centrifuged at 12000 × g at 4°C for 5 minutes, and the supernatants
628 were transferred to a 96-well black culture plate. Then, the samples and standards

were read with a Multimode Microplate Reader (Tecan Life Sciences). Finally, the ATP level was calculated according to the standard curve.

RNA sequencing and analysis

GV-stage oocytes were collected from three young, three aged and three CNP treated aged mice. mRNA samples were collected from 5 oocytes from the same mouse of each group. The mRNA was directly reverse-transcribed through oligo dT. The reverse-transcribed cDNA was amplified, and the cDNA was cut by Tn5 transposase digestion, and linkers were added to obtain the required sequencing library. The constructed library was entered into the sequencing program after passing through an Agilent 2100 Bioanalyzer and RT–PCR quality control. The PE100 sequencing strategy was used to assess gene expression changes at the transcription level. Dr. Tom（Dr. Tom is a web-based solution that offers convenient analysis, visualization, and interpretation of various types of RNA data，https://www.bgi.com/global/service/dr-tom）was used for difference analysis, GO analysis, KEGG analysis, and other analyses.

Reverse transcriptase quantitative PCR (RT-qPCR) analysis

Total RNA from oocytes was extracted using MiniBEST Universal RNA Extraction Kit (TaKaRa, Dalian, China), and reverse transcribed to synthesize cDNA using a PrimeScript RT Master Mix reverse transcription kit (TaKaRa) according to the manufacturer's instructions. RT-qPCR quantitation of mRNAs was performed using TB Green™ Premix Ex Taq™ II (TaKaRa) with Applied Biosystems

StepOnePlus Real-Time PCR System (Thermo Fisher Scientific, Massachusetts, USA) using the following parameters: 95 ℃ for 1 min, followed by 40 cycles at 95 ℃ for 5 s and 60 °C for 34 s. The PCR primers used in this study were shown in Table S1. Transcript levels were normalized to those of the housekeeping gene *Gapdh*. The CT value was used to calculate the fold change using the $2^{-\Delta\Delta Ct}$ method. Each experiment was repeated independently at least thrice.

Statistical analysis

Statistical analyses were performed using GraphPad Prism 8.00 software (GraphPad, CA, United States). Differences between two groups were assessed using the t-test. Data from at least three biological repeats were reported as means ± SEM. Results of statistically significant differences were denoted by asterisk. ($P < 0.05$ denoted by *, $P < 0.01$ denoted by **, $P < 0.001$ denoted by ***, and $P < 0.0001$ denoted by ****).

Ethics approval

The experimental protocols and mice handling procedures were reviewed and approved by the Institutional Animal Care and Use Committee of the College of Veterinary Medicine, Northwest A&F University (No. 2018011212).

Conflicts of interest

All of the contributing authors declared no conflicts of interest. All authors read and approved the final manuscript.

Data availability statement

All data is included in the manuscript and supporting information.

Acknowledgments

We thank other members in the Ma laboratory for their helpful discussion on the manuscript. This work was supported in part by National Natural Science Foundation of China (31772818).

References

Adhikari, D., Lee, I.-w., Yuen, W. S., & Carroll, J. (2022). Oocyte mitochondria—key regulators of oocyte function and potential therapeutic targets for improving fertility. *Biology of Reproduction, 106*(2), 366-377.

Akabane, S., Uno, M., Tani, N., Shimazaki, S., Ebara, N., Kato, H., . . . Oka, T. (2016). PKA regulates PINK1 stability and Parkin recruitment to damaged mitochondria through phosphorylation of MIC60. *Molecular cell, 62*(3), 371-384.

Amer, Y. O., & Hebert-Chatelain, E. (2018). Mitochondrial cAMP-PKA signaling: What do we really know? *Biochimica et Biophysica Acta (BBA)-Bioenergetics, 1859*(9), 868-877.

Arhin, S. K., Lu, J., Xi, H., & Jin, X. (2018). Energy requirements in mammalian oogenesis. *Cellular and Molecular Biology, 64*(10), 12-19.

Ateneo, F. S. (2019). Mitophagy and Oxidative Stress in Cancer and Aging: Focus on Sirtuins and Nanomaterials. *Journal: Oxidative Medicine and Cellular Longevity*, 1-19.

Bae, C.-R., Hino, J., Hosoda, H., Arai, Y., Son, C., Makino, H., . . . Nojiri, T. (2017). Overexpression of C-type natriuretic peptide in endothelial cells protects against insulin resistance and inflammation during diet-induced obesity. *Scientific reports, 7*(1), 1-13.

Bartimaeus, E.-A. S., Obi, C. E., Igwe, F. U., & Nwachuku, E. O. (2020). Impact of Age on Hormonal Profiles of Sub-Fertile Women Attending Fertility Clinic in Umuahia, Abia State, South Eastern Nigeria. *Open Journal of Internal Medicine, 10*(01), 51.

Bentov, Y., Yavorska, T., Esfandiari, N., Jurisicova, A., & Casper, R. F. (2011). The contribution of mitochondrial function to reproductive aging. *Journal of assisted reproduction and genetics, 28*(9), 773-783.

Broekmans, F., Soules, M., & Fauser, B. (2009). Ovarian aging: mechanisms and clinical consequences. *Endocrine reviews, 30*(5), 465-493.

Chang, E. M., Song, H. S., Lee, D. R., Lee, W. S., & Yoon, T. K. (2014). In vitro maturation of human oocytes: its role in infertility treatment and new possibilities. *Clinical and experimental reproductive medicine, 41*(2), 41.

Chiang, T., Schultz, R. M., & Lampson, M. A. (2011). Age-dependent susceptibility of chromosome cohesion to premature separase activation in mouse oocytes.

Biology of reproduction, 85(6), 1279-1283.

Combelles, C. M., Gupta, S., & Agarwal, A. (2009). Could oxidative stress influence the in-vitro maturation of oocytes? *Reproductive biomedicine online, 18*(6), 864-880.

Coticchio, G., Dal Canto, M., Mignini Renzini, M., Guglielmo, M. C., Brambillasca, F., Turchi, D., . . . Fadini, R. (2015). Oocyte maturation: gamete-somatic cells interactions, meiotic resumption, cytoskeletal dynamics and cytoplasmic reorganization. *Human Reproduction Update, 21*(4), 427-454.

De Gaetano, A., Gibellini, L., Zanini, G., Nasi, M., Cossarizza, A., & Pinti, M. (2021). Mitophagy and oxidative stress: The role of aging. *Antioxidants, 10*(5), 794.

Eichenlaub-Ritter, U. (2013). Oocyte ageing and its cellular basis. *International Journal of Developmental Biology, 56*(10-11-12), 841-852.

Eichenlaub-Ritter, U., Vogt, E., Yin, H., & Gosden, R. (2004). Spindles, mitochondria and redox potential in ageing oocytes. *Reproductive biomedicine online, 8*(1), 45-58.

Eichenlaub-Ritter, U., Wieczorek, M., Lüke, S., & Seidel, T. (2011). Age related changes in mitochondrial function and new approaches to study redox regulation in mammalian oocytes in response to age or maturation conditions. *Mitochondrion, 11*(5), 783-796.

FitzHarris, G., Marangos, P., & Carroll, J. (2007). Changes in endoplasmic reticulum structure during mouse oocyte maturation are controlled by the cytoskeleton and cytoplasmic dynein. *Developmental biology, 305*(1), 133-144.

Furnus, C. C., De Matos, D., Picco, S., García, P. P., Inda, A. M., Mattioli, G., & Errecalde, A. L. (2008). Metabolic requirements associated with GSH synthesis during in vitro maturation of cattle oocytes. *Animal reproduction science, 109*(1-4), 88-99.

Gandolfi, T. B., & Gandolfi, F. (2001). The maternal legacy to the embryo: cytoplasmic components and their effects on early development. *Theriogenology, 55*(6), 1255-1276.

Jiang, Y., Shen, M., Chen, Y., Wei, Y., Tao, J., & Liu, H. (2021). Melatonin represses mitophagy to protect mouse granulosa cells from oxidative damage. *Biomolecules, 11*(7), 968.

Jin, X., Wang, K., Wang, L., Liu, W., Zhang, C., Qiu, Y., . . . Yang, Z. (2022). RAB7 activity is required for the regulation of mitophagy in oocyte meiosis and oocyte quality control during ovarian aging. *Autophagy, 18*(3), 643-660.

Liu, M., Sims, D., Calarco, P., & Talbot, P. (2003). Biochemical heterogeneity, migration, and pre-fertilization release of mouse oocyte cortical granules. *Reproductive Biology and Endocrinology, 1*(1), 1-11.

Lobo, M. J., Reverte-Salisa, L., Chao, Y.-C., Koschinski, A., Gesellchen, F., Subramaniam, G., . . . Paolocci, E. (2020). Phosphodiesterase 2A2 regulates mitochondria clearance through Parkin-dependent mitophagy.

Communications biology, *3*(1), 1-16.

Ma, J.-Y., Li, S., Chen, L.-N., Schatten, H., Ou, X.-H., & Sun, Q.-Y. (2020). Why is oocyte aneuploidy increased with maternal aging? *Journal of genetics and genomics*, *47*(11), 659-671.

Mao, L., Lou, H., Lou, Y., Wang, N., & Jin, F. (2014). Behaviour of cytoplasmic organelles and cytoskeleton during oocyte maturation. *Reproductive biomedicine online*, *28*(3), 284-299.

Matsuda, N., Sato, S., Shiba, K., Okatsu, K., Saisho, K., Gautier, C. A., . . . Sato, F. (2010). PINK1 stabilized by mitochondrial depolarization recruits Parkin to damaged mitochondria and activates latent Parkin for mitophagy. *Journal of Cell Biology*, *189*(2), 211-221.

May-Panloup, P., Boucret, L., Chao de la Barca, J.-M., Desquiret-Dumas, V., Ferré-L'Hotellier, V., Morinière, C., . . . Reynier, P. (2016). Ovarian ageing: the role of mitochondria in oocytes and follicles. *Human Reproduction Update*, *22*(6), 725-743.

McClatchie, T., Meredith, M., Ouédraogo, M. O., Slow, S., Lever, M., Mann, M. R., . . . Baltz, J. M. (2017). Betaine is accumulated via transient choline dehydrogenase activation during mouse oocyte meiotic maturation. *Journal of Biological Chemistry*, *292*(33), 13784-13794.

Miao, Y., Cui, Z., Gao, Q., Rui, R., & Xiong, B. (2020). Nicotinamide mononucleotide supplementation reverses the declining quality of maternally aged oocytes. *Cell reports*, *32*(5), 107987.

Mikwar, M., MacFarlane, A. J., & Marchetti, F. (2020). Mechanisms of oocyte aneuploidy associated with advanced maternal age. *Mutation Research/Reviews in Mutation Research*, 108320.

Miyazaki, S., & Ito, M. (2006). Calcium signals for egg activation in mammals. *Journal of pharmacological sciences*, *100*(5), 545-552.

Moyes, A. J., & Hobbs, A. J. (2019). C-type natriuretic peptide: a multifaceted paracrine regulator in the heart and vasculature. *International journal of molecular sciences*, *20*(9), 2281.

Narendra, D. P., & Youle, R. J. (2011). Targeting mitochondrial dysfunction: role for PINK1 and Parkin in mitochondrial quality control. *Antioxidants & redox signaling*, *14*(10), 1929-1938.

Pan, M.-H., Wu, Y.-K., Liao, B.-Y., Zhang, H., Li, C., Wang, J.-L., . . . Ma, B. (2021). Bisphenol A Exposure Disrupts Organelle Distribution and Functions During Mouse Oocyte Maturation. *Frontiers in Cell and Developmental Biology*, *9*, 656.

Peake, N., Hobbs, A., Pingguan-Murphy, B., Salter, D., Berenbaum, F., & Chowdhury, T. (2014). Role of C-type natriuretic peptide signalling in maintaining cartilage and bone function. *Osteoarthritis and cartilage*, *22*(11), 1800-1807.

792 Reader, K. L., Stanton, J.-A. L., & Juengel, J. L. (2017). The role of oocyte organelles
793 in determining developmental competence. *Biology, 6*(3), 35.

794 Richani, D., & Gilchrist, R. B. (2022). Approaches to oocyte meiotic arrest in vitro
795 and impact on oocyte developmental competence. *Biology of Reproduction,*
796 *106*(2), 243-252.

797 Russ, J. E., Haywood, M. E., Lane, S. L., Schoolcraft, W. B., & Katz-Jaffe, M. G.
798 (2022). Spatially resolved transcriptomic profiling of ovarian aging in mice.
799 *Iscience, 25*(8), 104819.

800 Sato, Y., Cheng, Y., Kawamura, K., Takae, S., & Hsueh, A. J. (2012). C-type
801 natriuretic peptide stimulates ovarian follicle development. *Molecular*
802 *endocrinology, 26*(7), 1158-1166.

803 Schuel, H. (1978). Secretory functions of egg cortical granules in fertilization and
804 development: A critical review. *Gamete Research, 1*(3-4), 299-382.

805 Schwarzer, C., Siatkowski, M., Pfeiffer, M. J., Baeumer, N., Drexler, H., Wang, B., . .
806 . Boiani, M. (2014). Maternal age effect on mouse oocytes: new biological
807 insight from proteomic analysis. *Reproduction, 148*(1), 55-72.

808 Shen, M., Jiang, Y., Guan, Z., Cao, Y., Sun, S.-c., & Liu, H. (2016). FSH protects
809 mouse granulosa cells from oxidative damage by repressing mitophagy.
810 *Scientific reports, 6*(1), 1-13.

811 Shen, Q., Liu, Y., Li, H., & Zhang, L. (2021). Effect of mitophagy in oocytes and
812 granulosa cells on oocyte quality. *Biology of Reproduction, 104*(2), 294-304.

813 Soto-Heras, S., & Paramio, M.-T. (2020). Impact of oxidative stress on oocyte
814 competence for in vitro embryo production programs. *Research in Veterinary*
815 *Science.*

816 Soto-Heras, S., Paramio, M.-T., & Thompson, J. G. (2019). Effect of pre-maturation
817 with C-type natriuretic peptide and 3-isobutyl-1-methylxanthine on cumulus-
818 oocyte communication and oocyte developmental competence in cattle.
819 *Animal reproduction science, 202*, 49-57.

820 Sun, M.-H., Li, X.-H., Xu, Y., Xu, Y., Pan, Z.-N., & Sun, S.-C. (2020). Citrinin
821 exposure disrupts organelle distribution and functions in mouse oocytes.
822 *Environmental research, 185*, 109476.

823 Watson, A. (2007). Oocyte cytoplasmic maturation: a key mediator of oocyte and
824 embryo developmental competence. *Journal of animal science, 85*(suppl_13),
825 E1-E3.

826 Wei, Q., Zhou, C., Yuan, M., Miao, Y., Zhao, X., & Ma, B. (2017). Effect of C-type
827 natriuretic peptide on maturation and developmental competence of immature
828 mouse oocytes in vitro. *Reproduction, Fertility and Development, 29*(2), 319-
829 324.

830 Xi, G., Wang, W., Fazlani, S. A., Yao, F., Yang, M., Hao, J., . . . Tian, J. (2019). C-type
831 natriuretic peptide enhances mouse preantral follicle growth. *Reproduction,*
832 *157*(5), 445-455.

833 Zarkovic, N. (2020). Roles and Functions of ROS and RNS in Cellular Physiology
834 and Pathology. In (Vol. 9, pp. 767): MDPI.

835 Zhang, H., Lu, S., Xu, R., Tang, Y., Liu, J., Li, C., . . . Wei, Q. (2020). Mechanisms of
836 estradiol-induced EGF-like factor expression and oocyte maturation via G
837 protein-coupled estrogen receptor. *Endocrinology, 161*(12), bqaa190.

838 Zhang, M., Lu, Y., Chen, Y., Zhang, Y., & Xiong, B. (2020). Insufficiency of
839 melatonin in follicular fluid is a reversible cause for advanced maternal age-
840 related aneuploidy in oocytes. *Redox biology, 28*, 101327.

841 Zhang, M., Su, Y.-Q., Sugiura, K., Wigglesworth, K., Xia, G., & Eppig, J. J. (2011).
842 Estradiol promotes and maintains cumulus cell expression of natriuretic
843 peptide receptor 2 (NPR2) and meiotic arrest in mouse oocytes in vitro.
844 *Endocrinology, 152*(11), 4377-4385.

845 Zhang, M., Su, Y.-Q., Sugiura, K., Xia, G., & Eppig, J. J. (2010). Granulosa cell
846 ligand NPPC and its receptor NPR2 maintain meiotic arrest in mouse oocytes.
847 *Science, 330*(6002), 366-369.

848 Zhang, T., Xi, Q., Wang, D., Li, J., Wang, M., Li, D., . . . Jin, L. (2019). Mitochondrial
849 dysfunction and endoplasmic reticulum stress involved in oocyte aging: an
850 analysis using single-cell RNA-sequencing of mouse oocytes. *Journal of*
851 *ovarian research, 12*(1), 1-9.

852 Zhenwei, J., & Xianhua, Z. (2019). Pre-IVM treatment with C-type natriuretic peptide
853 in the presence of cysteamine enhances bovine oocytes antioxidant defense
854 ability and developmental competence in vitro. *Iranian journal of veterinary*
855 *research*, *20*(3), 173.

856

857

Figure legends

Figure1. Effects of CNP supplementation on the oocyte quality and female fertility in aged mice. (A) A timeline diagram of CNP administration and superovulation. (B) Representative images of young, aged and CNP administration aged (Aged + CNP) mice as well as their ovaries. (C) Body weights of young, aged and aged + CNP aged mice. (D) Ovarian weights of young, aged and aged + CNP mice. (E) Ratios of ovarian weight to body weight for each group of mice. (F) Serum CNP concentrations were measured in young, aged, and aged + CNP mice. (G) Representative images of the oocyte polar body extrusion in young, aged, and aged + CNP mice. Scale bar: 100 μm. (H) Ovulated oocytes were counted in young, aged, and aged + CNP mice. (I) Rate of polar body extrusion in young, aged, and aged + CNP mice. (J) The rate of fragmented oocytes was recorded in young, aged, and aged + CNP mice. (K) Representative images of ovarian sections from young, aged, and aged+CNP mice. Scale bars: 100 μm. (L) Follicles at different developmental stages were counted in young, aged, and aged+CNP ovaries. (M) Average litter size of mated mice was assessed by mating with two-months old male mice.

Figure2. CNP supplementation recovers cytoplasmic maturation events of maternally aged mouse oocytes. (A) Representative images of the spindle morphology and chromosome alignment at metaphase II in young, aged, and aged + CNP mice. Scale bar, 10 μm. (B) The rate of aberrant spindles at metaphase II was recorded in young, aged, and aged + CNP mice. (C) Representative images of the Golgi apparatus distribution at metaphase II in young, aged, and aged + CNP mice. Scale bar, 10 μm. (D) The rate of aberrant Golgi apparatus distribution was recorded in young, aged, and aged + CNP mice. (E) Representative images of the endoplasmic reticulum distribution at metaphase II in young, aged, and aged + CNP mice. Scale bar, 10 μm. (F) The rate of aberrant endoplasmic reticulum distribution was recorded in young, aged, and aged + CNP mice. (G) Representative images of the cortical granules (CGs) distribution in young, aged, and aged + CNP mice. Scale bar, 10 μm. (H) The rate of mislocalized CGs was recorded in the young, aged, and aged + CNP mice. (I) The fluorescence intensity of CG signals was measured in the young, aged, and aged + CNP mice oocyte. (J) Representative images of mitochondrial distribution in the young, aged, and aged + CNP mice oocytes stained with MitoTracker Red. Scale bar, 10 μm. (K) The abnormal rate of mitochondrial distribution was recorded in

the young, aged, and aged + CNP mice oocytes. (L) ATP levels were measured in the young, aged, and aged + CNP mice. (M) Mitochondrial membrane potential (ΔΨm) was detected by JC-1 staining in in the young, aged, and aged + CNP mice oocytes. Scale bar, 10 μm. (N) The ratio of red to green fluorescence intensity was calculated in the young, aged, and aged + CNP mice oocytes.

Figure 3. Effects of CNP on the ROS content, DNA damage, and apoptosis in aged oocytes. (A) Representative images of ROS levels detected by DCFH staining in the young, aged, and aged + CNP mice oocytes. Scale bar, 100 μm. (B) The fluorescence intensity of ROS signals was measured in the young, aged, and aged + CNP mice oocytes. (C) Oocyte NADPH levels in the young, aged, and aged + CNP mice were measured. (D) The ratio of GSH/GSSG was measured in the young, aged, and aged + CNP mice oocytes. (E) Representative images of DNA damage stained with the γ-H2AX antibody in young, aged, and aged + CNP oocytes. Scale bar, 10 μm. (F) γ-H2AX fluorescence intensity was counted in young, aged, and aged + CNP oocytes. (G) Representative images of apoptotic status, assessed by Annexin-V staining, in young, aged, and aged + CNP oocytes. Scale bar, 20 μm. (H) The fluorescence intensity of Annexin-V signals was measured in young, aged, and aged + CNP oocytes.

Figure 4. Effects of CNP on the fertilization ability and embryonic development of aged oocytes. (A) Representative images of early embryos developed from young, aged, and aged + CNP oocytes in vitro fertilization. Scale bar, 100 μm. (B) The fertilization rate (2 cell embryos rate), (C) 4 cell embryos rate, (D) 8 cell embryos rate, (E) morula rate and (F) blastocyst formation rates were recorded in the young, aged, and aged + CNP groups. Data in (B)–(F) are presented as mean percentage (mean ± SEM) of at least three independent experiments.

Figure 5. Effect of CNP supplementation on transcriptome profiling of aged oocytes

(A) Heatmap illustration displaying gene expression of young, aged, and aged+ CNP oocytes. (B) Volcano plot showing differentially expressed genes (DEGs; downregulated, blue; upregulated, red) in Young vs Aged oocytes. Some highly DEGs are listed. (C) Volcano plot showing DEGs in Aged vs Aged + CNP oocytes. Some

highly DEGs are listed. (D) KEGG enrichment analysis of upregulated and downregulated DEGs in Young vs Aged oocytes. (E) KEGG enrichment analysis of upregulated and downregulated DEGs in Aged vs Aged + CNP oocytes.

Figure 6. Evaluation of CNP supplementation on mitophagy activity of aged oocytes. (A) Representative images of mitochondria morphology and structure in young, aged, and aged + CNP oocytes by TEM. (B) Accumulation of mitochondria damage in young, aged, and aged + CNP oocytes. Under TEM images, percentages of damaged mitochondria per area (500 nm × 500 nm) were shown. At least 4 visions were chosen and mitochondria were counted by two individuals. (C) Representative images of mitochondria ROS stained with MitoSOX in young, aged, aged + CNP oocytes. Scale bar, 20 μm. (D) Fluorescence intensity of MitoSOX signals was measured in young aged, aged + CNP oocytes. (E) Western blots of P62, LC3-I/II, PINK1 and Parkin in young, aged, and aged + CNP oocytes. GAPDH was used as internal control. (F-I) Relative gray value of proteins detected with western blots as compared with controls. (J) Oocyte cAMP concentrations were measured in young, aged, and aged + CNP mice. (K) Representative images at day 0, day 2, day 4 and day 6 of cultured preantral follicles with or without CNP or CNP+H89 treatment. Scale bar=50μm. (L) Diameters of preantral follicles with or without CNP or CNP+H89 treatment from day 0 to day 6. Six independent culture experiments were performed. (M) Western blots of PINK1 and Parkin in aged, aged + CNP and aged + CNP+H89 treated oocytes. GAPDH was used as internal control. (N-O) Relative gray value of proteins detected with western blots as compared with controls. (P) Double immunofluorescence staining of Parkin and TOMM20. The mitochondria outer membrane protein TOMM20 was performed to reveal the translocation of PRKN proteins on mitochondria. Red, PRKN; Green, TOMM20; Blue, DNA was labeled with Hoechst 33342. Bar: 20 μm. (Q) The colocalization of Parkin and TOMM20 in oocytes from aged, aged + CNP and aged + CNP+H89 treated mice were compared. Pearson,s R shows the results of co-location analysis.

Figure 1

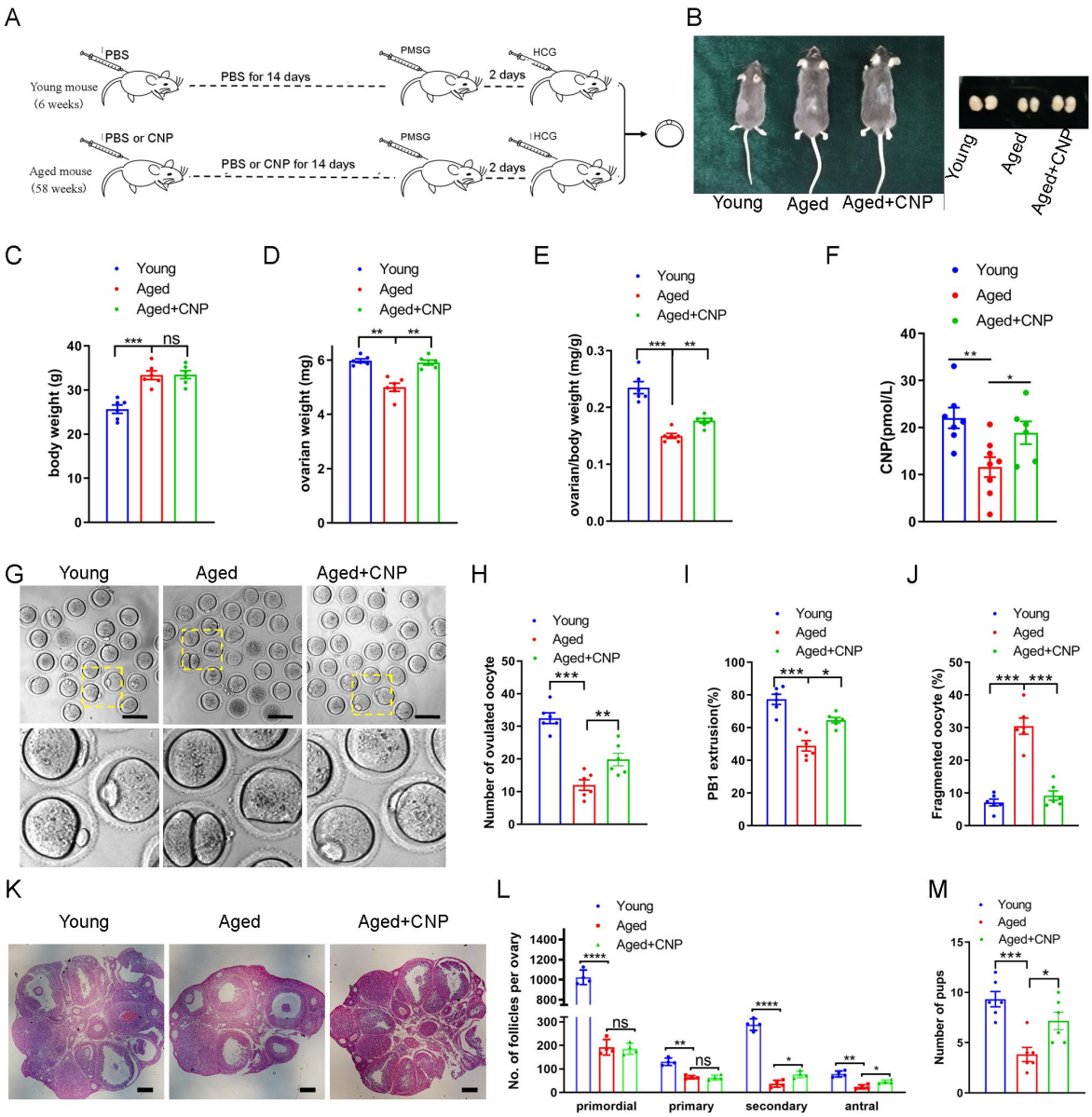

Figure 2

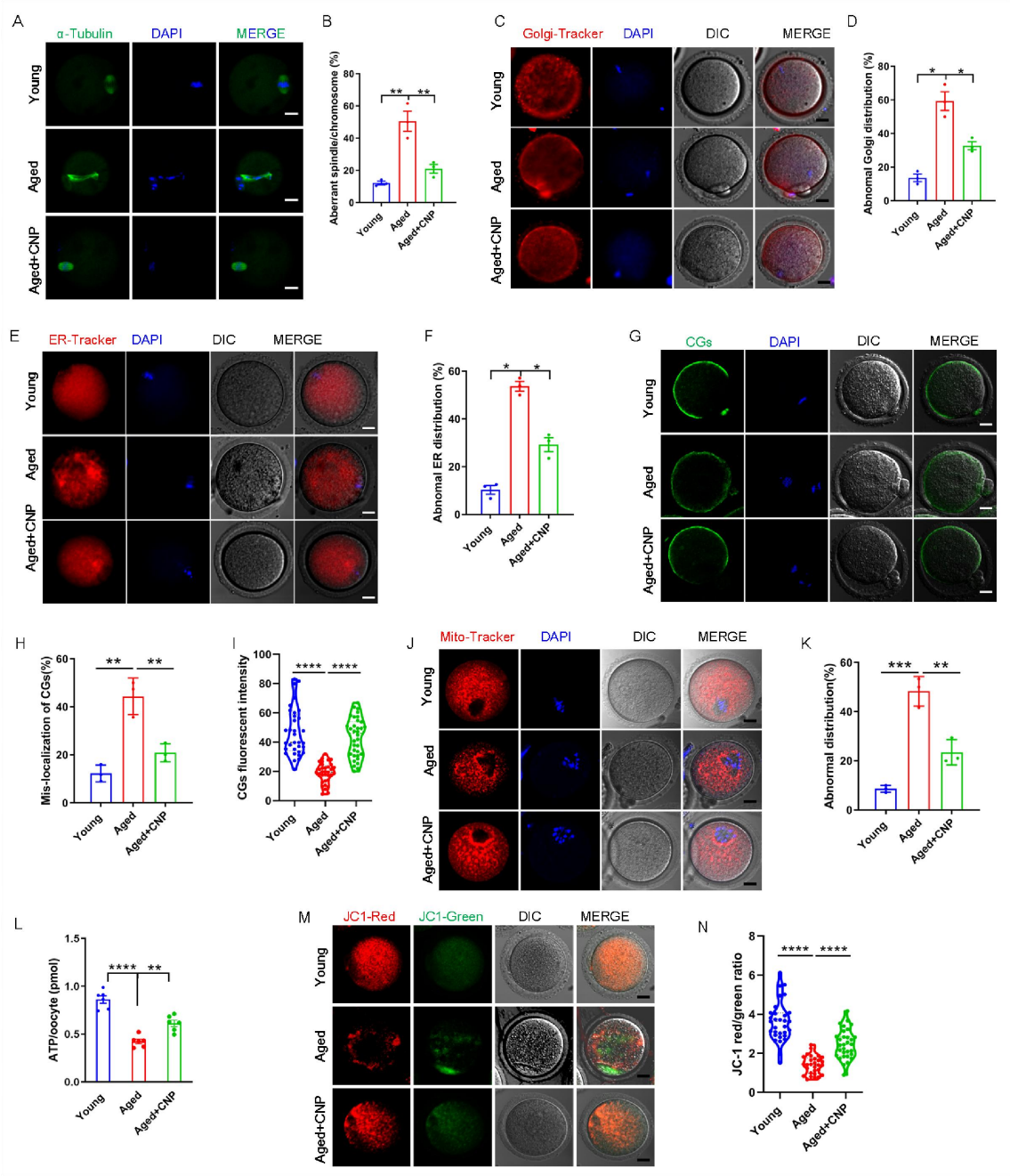

Figure 3

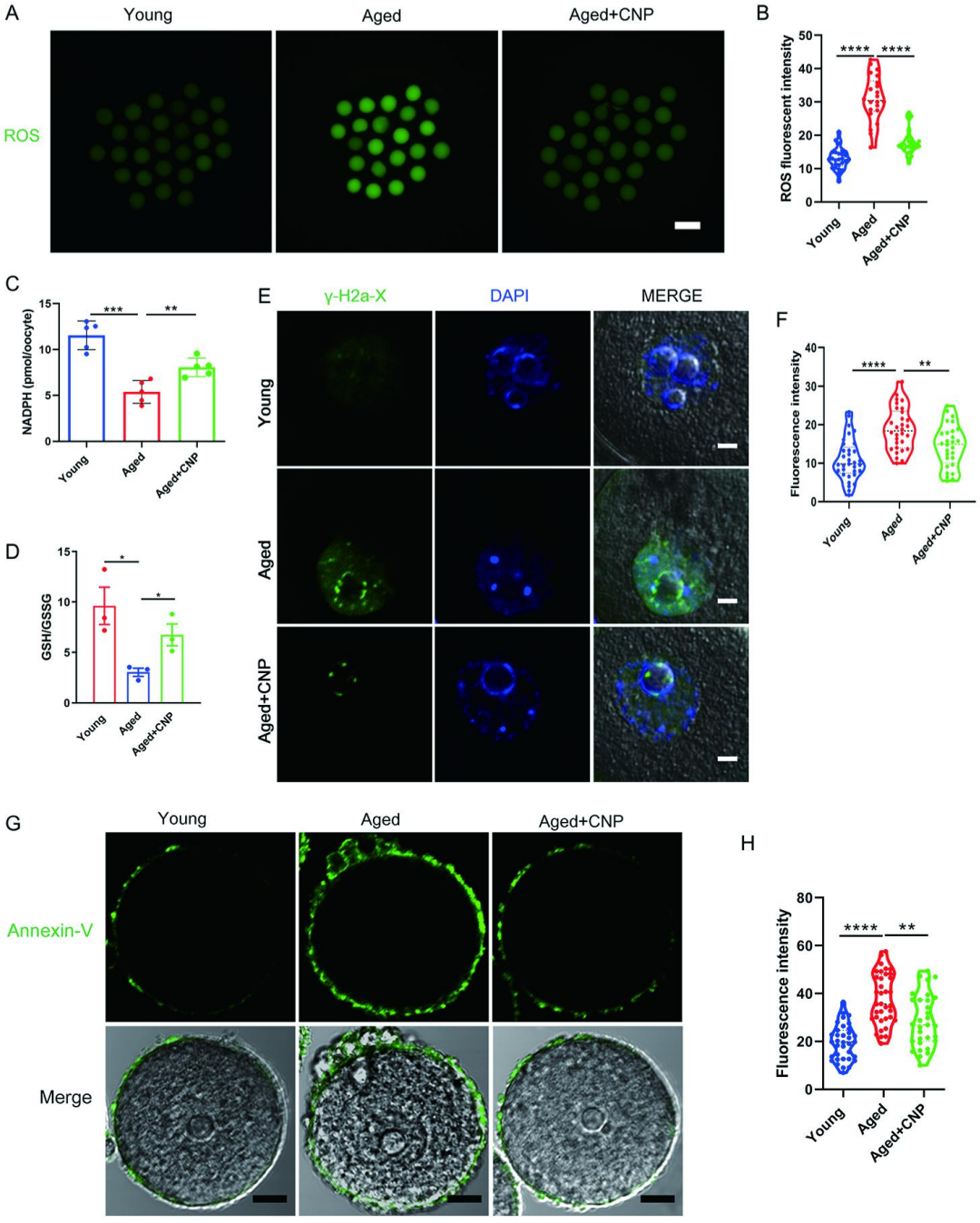

Figure 4

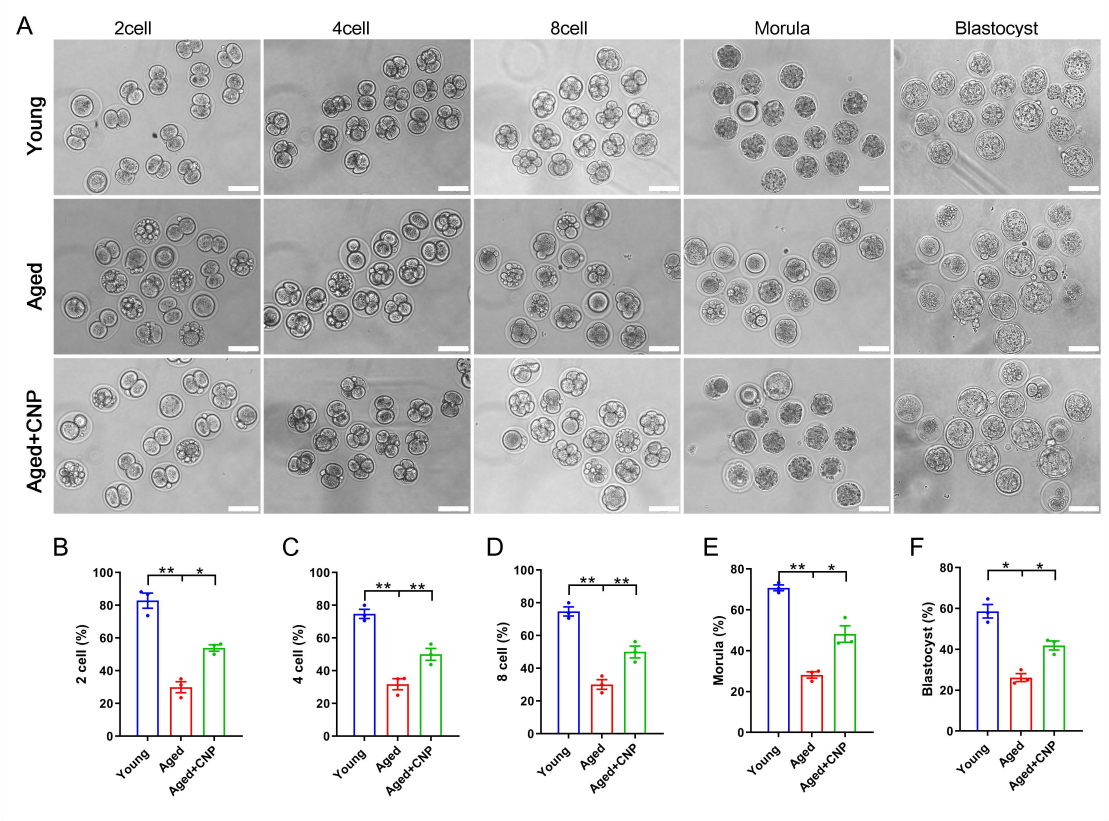

Figure 5

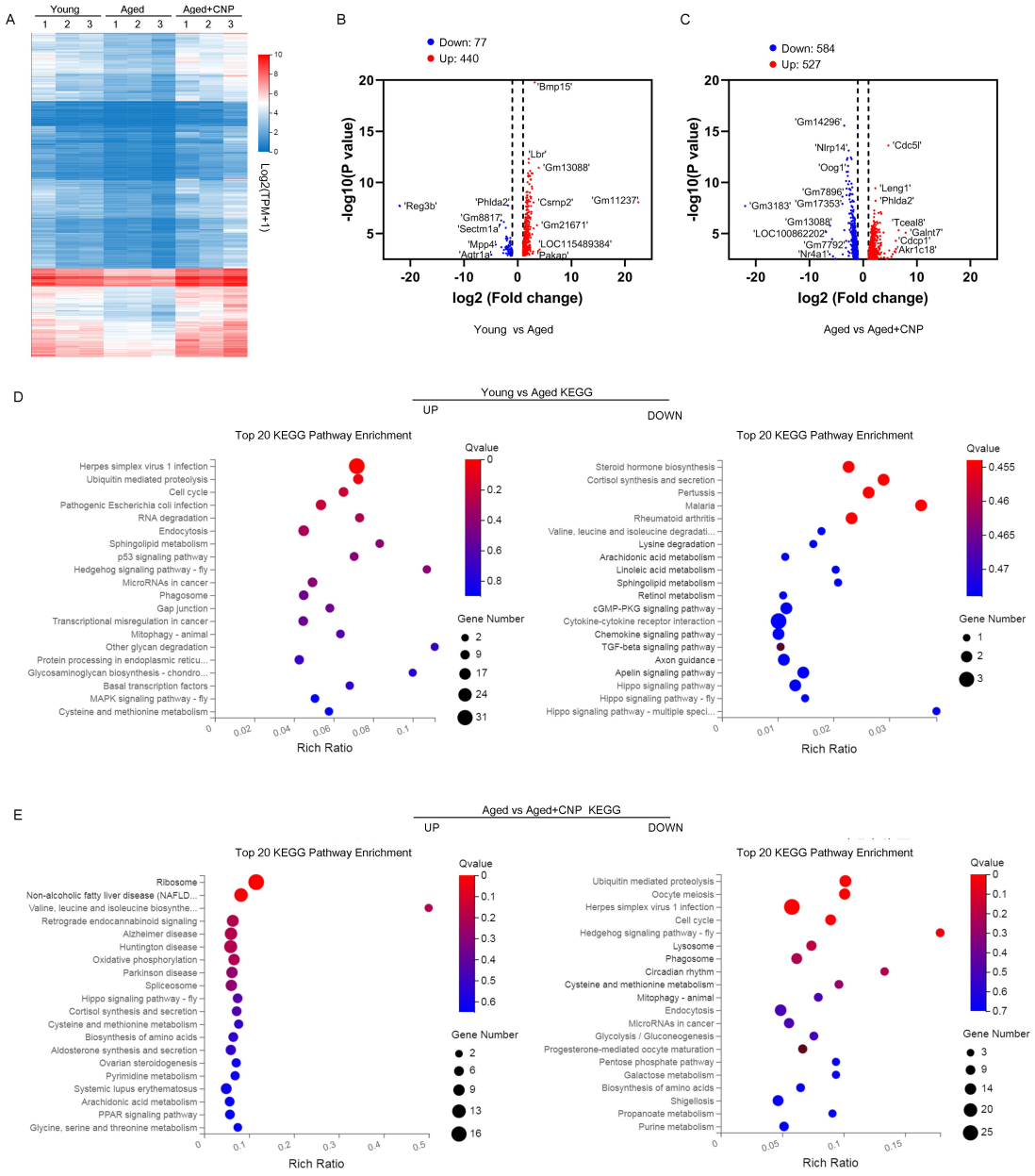

Figure 6